Springer

Journal of
Mechanical
Science and
Technology

Journal of Mechanical Science and Technology 23 (2009) 302~310

www.springerlink.com/content/1738-494x
DOI 10.1007/s12206-009-0107-z

Fault detection and isolation of DURUMI-II using similarity measure †

WookJe Park[1], Sang H. Lee[2,*] and JungIl Song[2]

[1]*Department of Mechanical and Aeronautical Engineering, Western Michigan University, Kalamazoo, MI 49008*
[2]*School of Mechatronics, Changwon National University 9 Sarim-dong, Changwon, 641-773, Korea*

(Manuscript Received January 25, 2008; Revised December 15, 2008; Accepted January 13, 2009)

Abstract

This paper describes the flight test method for studying the primary control surface stuck condition and the combination stuck of the primary control. An aircraft must show controllability and trimmability under post-failure conditions. An aircraft is successfully tested under various fault conditions. It is recognized that a control surface fault is detected by monitoring the value of the coefficients related to the control surface deviation. The control surface stuck position is determined by comparing the trim value with the reference value. To detect and isolate the fault, an analysis that employs the real-time parameter estimation method is used. If the flight control system is reconfigured using online estimates of aircraft parameters from a real-time parameter estimation scheme, the reliability increases without the addition of sensors or additional cost.

Keywords: Fault detection and isolation; Real-time parameter estimation; Control surface stuck; Flight test; UAV

1. Introduction

When a control surface malfunction occurs during a flight, the flight control system usually has redundancy for enhancing the safety of the damaged aircraft. If the status of the damage is known after the occurrence of the failure, a fault-tolerant control system is capable of adapting to the various faults in real time. Therefore, the pilot (or the flight control system) accomplishes the mission (or returns to a safe region). The fault-tolerant control system is required to perform fault detection and isolation (FDI) following the failure of a critical system [1]. The conventional FDI methods are the hardware method and the analytical method [2]. In the hardware method, parity equations, hardware, and redundancy sensors are used for a modern aircraft. In the analytical method, a residual approach and parameter estimation are used for studying the flight dynamics. To implement a failure strategy, a variety of control surfaces, including primary control surfaces, speed brakes, wing flaps, and spoilers, a flight control computer (FCC), and thrust mechanisms can be used [3-4]. Assuming the controllability and trimmability of the aircraft under post-failure conditions, in the event of control surface stuck, the aircraft can continue flying with the help of the FCC, which has restructured and reconfigured controllers for different grades of system failure. For determining or analyzing the fault cases, statistical information on elevator deflection, aileron deflection, and other parameters has been studied. However, malfunctions could be invoked through processing overlapping data, simple mean, or other statistical information. Fault data can be obtained from the measurements through statistical analysis, pattern recognition, or other methods. However, these methods are not that effective because of the occurrence of data mixing or the necessity of higher dimensional partitioning. Hence, we propose a similarity measure that represents the degree of similarity between two or more sets.

In particular, reliable input data invoke reliable ones; hence it is required to process data that have the

† This paper was recommended for publication in revised form by Associate Editor Eung-Soo Shin

* Corresponding author. Tel.: +82 55 213 3884, Fax.: +82 55 267 5142
E-mail address: leehyuk@changwon.ac.kr

minimum uncertainty. It is well known that entropy implies the uncertainty of the data. Entropy has been studied in several fields such as information theory, thermodynamics, and system theory. The entropy of a fuzzy set has been studied by numerous researchers [5-7]. However, we have noted that a reliable result cannot be obtained by using only the fuzzy entropy value [5]. This controversial issue should be resolved by an altogether different approach; hence, we propose the similarity measure. In this paper, we explain the properties of certainty, uncertainty, similarity, and unsimiliarity. The proposed similar measure is explained through the aforementioned properties of certainty and uncertainty. The similarity measures are designed on the basis of a distance measure. By using this similarity measure, we do data processing, and the reliable data obtained are recorded.

Without adding a sensor or any additional cost, there is an increase in reliability when the flight control system is reconfigured by using the online estimates of aircraft parameters through a real-time parameter estimation scheme. This study deals with the failure of primary control surfaces (elevators, ailerons, and rudders). The real-time parameter estimation method, which is an analytic method, is adopted [8-9].

In the next section, we introduce the airplane model and flight test circumstances. In Section 3, we discuss the parameter estimation and similarity measure construction for the proper detection of faults. Furthermore, the fault decision algorithm and discussions on the experimental data are also provided. Finally, the conclusions are given in Section 4.

2. Modeling and flight test

In this section, we derive the airplane model and the flight test condition. The estimation procedures are introduced with the help of well known airplane dynamics. Discussions on the control surface struck condition and the flight test procedure are also included.

2.1 Airplane model

For aircraft dynamics along a combination of the longitudinal and lateral directions combining aircraft dynamics, x and u denote the state vector and elevator control input variable, respectively. The output vector y is defined by using x [10]

$$x = [\alpha \quad u \quad q \quad \theta \quad \beta \quad p \quad r \quad \phi]^T \tag{1}$$

and

$$u = \delta_e . \tag{2}$$

In the state vector, p,q,r are the angular velocities; α is the angle of attack; β denotes the sideslip angle; $u = \delta_e$ is the elevator deflection; and finally, ϕ,θ,ψ represent the roll, pitch, yaw angles, respectively. The elements of the system matrix can be derived from dynamics equations that are linearized by using small disturbance theory. In the steady flight condition, it is assumed that the motion of the airplane involves small deviations [11]. The system matrix and input matrix that contain the model parameters are represented by

$$A = \begin{bmatrix} A_1 & \vdots & 0 \\ \cdots & & \cdots \\ 0 & \vdots & A_2 \end{bmatrix} \tag{3}$$

and

$$B_e = [X_{\delta_e} \quad \frac{Z_{\delta_e}}{u_0} \quad M_{\delta_e} + \frac{M_{\dot{\alpha}}}{u_0} Z_{\delta_e} \quad 0 \ \vdots \ Y_{\delta_e} \quad L_{\delta_e} \quad N_{\delta_e} \quad 0]^T . \tag{4}$$

In (3), A_1 and A_2 are satisfied as follows:

$$A_1 = \begin{bmatrix} X_u & X_\alpha & 0 & -g\cos\theta_0 \\ \frac{Z_u}{u_0} & \frac{Z_\alpha}{u_0} & 1 & 0 \\ M_u + \frac{M_{\dot{\alpha}}}{u_0} Z_u & M_\alpha + \frac{M_{\dot{\alpha}}}{u_0} Z_\alpha & M_q + M_{\dot{\alpha}} & 0 \\ 0 & 0 & 1 & 0 \end{bmatrix}$$

and

$$A_2 = \begin{bmatrix} Y_v & Y_p & Y_r & g\cos\theta_0 \\ L_v^* + \frac{I_{xz}}{I_{xx}} N_v^* & L_p^* + \frac{I_{xz}}{I_{xx}} N_p^* & L_r^* + \frac{I_{xz}}{I_{xx}} N_r^* & 0 \\ N_v^* + \frac{I_{xz}}{I_{zz}} L_v^* & N_p^* + \frac{I_{xz}}{I_{zz}} L_p^* & N_r^* + \frac{I_{xz}}{I_{zz}} L_r^* & 0 \\ 0 & 1 & 0 & 0 \end{bmatrix}.$$

From (1) to (4), the following finite dimensional airplane dynamics are represented in the form of a state space equation [12-15].

$$\dot{x}(t) = Ax(t) + Bu(t) \tag{5}$$

$$y(t) = Cx(t) + Du(t) . \tag{6}$$

In (6), it is generally considered that $C = \mathrm{I}$ and $D = 0$. To estimate the parameters, Fourier transfor-

mation and the least squares method are used. The estimated parameters are assumed to be constant during flight test maneuvering [16].

By applying the Fourier transform to (5) and (6), we obtain

$$j\omega\,\tilde{x}(\omega) = A\tilde{x}(\omega) + B\tilde{u}(\omega) \tag{7}$$

$$\tilde{y}(\omega) = C\tilde{x}(\omega) + D\tilde{u}(\omega)\,. \tag{8}$$

For the k -th state equation of vector (7), the cost function is

$$J_k = \frac{1}{2}\sum_{n=1}^{m}\left| j\omega_n\,\tilde{x}(\omega_n) - A_k\tilde{x}(\omega_n) - B_k\tilde{u}(\omega_n)\right|^2 \tag{9}$$

The least squares cost function is

$$J = \frac{1}{2}\left(Y - X\Theta\right)^*\left(Y - X\Theta\right) \tag{10}$$

$$\hat{\Theta} = \left[\mathrm{Re}\left(X^*X\right)\right]^{-1}\mathrm{Re}\left(X^*Y\right) \tag{11}$$

where Y is the vector to be measured, X is a matrix of independent variables that denotes the given flight point. Here, X and Y are derived by applying the Fourier transform to (6), *i.e.*, $Y = X\Theta + \varepsilon$, where $\hat{\Theta}$ is a parameter vector, and ε is a complex error vector. The discrete Fourier transform for the i -th sampling time is obtained as $X_i(\omega) = X_{i-1}(\omega) + x_i e^{-j\omega_n\Delta t}$, where $e^{-j\omega_n\Delta t}$ is constant for a given frequency and constant sampling interval. Furthermore, the estimated parameter covariance matrix is

$$\mathrm{cov}\left(\hat{\Theta}\right) = E\left[\left(\hat{\Theta}-\Theta\right)\left(\hat{\Theta}-\Theta\right)^{-1}\right] = \hat{\sigma}^2\left[\mathrm{Re}\left(X^*X\right)\right]^{-1}$$

where, the equation error variance $\hat{\sigma}^2$ can be estimated from the residual $\hat{\sigma}^2 = \left[\left(Y - X\hat{\Theta}\right)^*\left(Y - X\hat{\Theta}\right)\right]/(m-p)$, where p is the number of parameters to be estimated, and m is the number of frequency points of interest.

In this study, a frequency spacing of 0.02 Hz was found to be adequate, which leads to 50 frequencies being evenly distributed in the interval 0.02-1.0 Hz for each transformed time-domain signal.

2.2 Control surface stuck condition and test procedure

Control surface failure is related to the stuck condition of elevator, rudder, and aileron. To fix the elevator, the one-piece elevator is split into two. To fix the rudder, the rudder is added [10]. To cause the control surface failure, the right elevator failure, the left rudder failure, and the left aileron failure and a combination of these failures can be used. The flight test is performed by excluding the uncontrollability and untrimmability of the aircraft under post-failure conditions; a flight test is scheduled. Table 1 shows the flight test conditions for control surface stuck.

Table 1. Control surface stuck conditions

Control Surface Stuck	Stuck Angle (deg)
Right Elevator	-10, -5, 0, +5, +10
Right Elevator +Left Rudder	-5, 0, +5 (at Left Rudder Stuck Angle : -10, -5, 0, +5, +10)

Fig. 1. DURUMI-II in take-off.

In the first flight test, the control input for the real-time parameter estimation is applied by using the knob and switching method [10]. The flight data is acquired for exciting the aircraft dynamics by using the abovementioned method [10, 16]. However, the applied time interval is found to be slightly inaccurate. To realize a constant control input and time interval, in the second stage of the flight test, the control input device is modified to use an RF modem and an R/C transmitter. Depending on the flight condition of the control surface stuck, the flight test engineer helps the aircraft in adapting to the control surface stuck. After the ground test, the pilot maintains the trimmed level flight under the post-failure condition; the engineer applies the control input by using a new device.

3. Parameter estimation and similarity measure

3.1 Parameter estimation for longitudinal mode

Considering the primary control of surface stuck and combination stuck, the aircraft must show controllability and trimmability under post-failure condi-

tions; Fig. 1 shows DURUMI-II during takeoff for the flight test. The flight test procedure involves the recovery of the aircraft from the fault state to the normal state [17]. Table 2 shows that the DURUMI-II is successfully tested under fault conditions. Further, the tables show the trim value of the available primary control surface under post-failure conditions.

In the longitudinal mode, in order to obtain the failure status of the elevator, the following data are required: the pitching moment coefficient with changes in the elevator deflection $C_{m_{\delta e}}$, change in the pitching moment coefficient with the angle of attack C_{m_α}, and change in the lift coefficient with the angle of attack C_{L_α}. The analysis of $C_{m_{\delta e}}$, C_{m_α}, and C_{L_α} is essential to obtain information on the aircraft performance characteristics. Fig. 2 shows the scatter diagram of $C_{m_{\delta e}}$, C_{m_α}, and C_{L_α}. Data points are dotted for the case of normal or elevator and rudder fixed simultaneously. We have listed the conditions of the data points with operating explanations in Fig. 2. Conventionally, statistical information such as mean and variance is commonly used. However, the analysis results of the stability and controllability derivatives do not clearly explain whether or not the control surface of the aircraft is normal because the standard deviation of the estimated results is large and the results are scattered. Hence, the proper detection or partitioning measures are required to classify the difference between the normal states and the post-failure states.

Table 2. Elevator trim value in longitudinal mode.

Normal Mode	5.7524	Rudder Stuck Angle				
Elevator Stuck Angle	Elevator Stuck Only	-10	-5	0	+5	10
-10	12.6396					
-5	10.1727		11.2178	10.1727		
0	5.7959	-5.0983	1.0060	5.7959	8.8797	14.7186
5	-1.7955	-10.0083	-9.1502	-1.7955	3.0761	
10	-9.8977					

Table 3. Operation conditions.

Mean	Mean of control surface normal condition
Normal	Control surface normal condition
ep10	Fixed Angle : Elevator $+10^0$
ep5	Fixed Angle : Elevator $+5^0$
ep0	Fixed Angle : Elevator 0^0
en5	Fixed Angle : Elevator -5^0
en10	Fixed Angle : Elevator -10^0
e0rl10	Fixed Angle : Elevator 0^0, Rudder Left 10^0
e0rl5	Fixed Angle : Elevator 0^0, Rudder Left 5^0
e0rr5	Fixed Angle : Elevator 0^0, Rudder Right 5^0
e0rr10	Fixed Angle : Elevator 0^0, Rudder Right ^{0}
en5rl5	Fixed Angle : Elevator -5^0, Rudder Left 5^0
en5rr5	Fixed Angle : Elevator -5^0, Rudder Right 5^0
ep5rl10	Fixed Angle : Elevator $+5^0$, Rudder Left 10^0
ep5rl5	Fixed Angle : Elevator $+5^0$, Rudder Left 5^0
ep5rr5	Fixed Angle : Elevator $+5^0$, Rudder Right 5^0

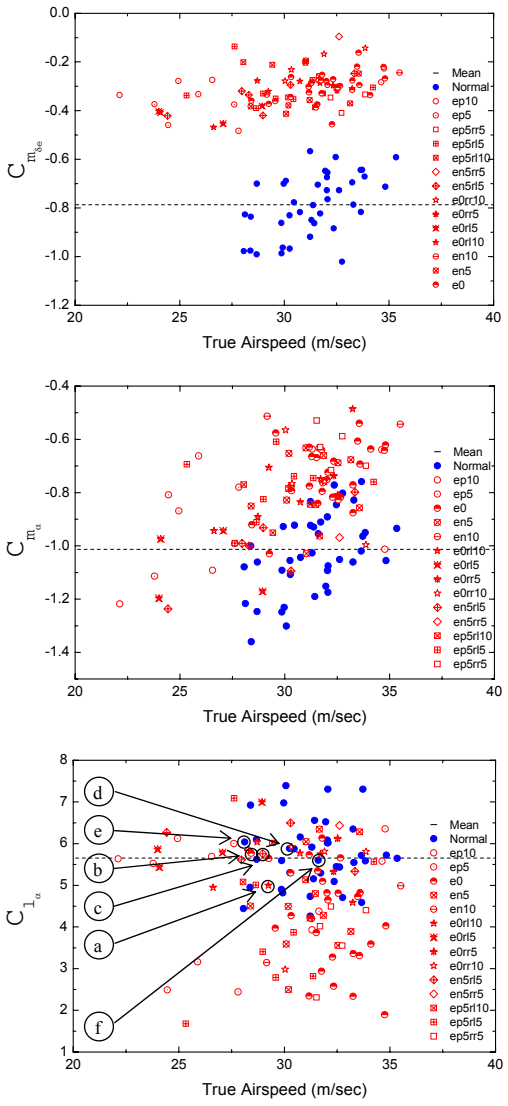

Fig. 2. Scatter diagram of $C_{m_{\delta e}}$, C_{m_α}, and C_{L_α} coefficients.

3.2 Similarity measure

To obtain the difference or similarity measure from $C_{m_{\delta e}}$, C_{m_α}, and C_{L_α}, we must design a proper measure. Measuring the similarity between two data sets is useful to decide whether both the data sets belong to the same group. With the help of the fuzzy entropy theory that is applicable to the uncertain data obtained, we have derived a similarity measure that is complementary to fuzzy entropy in meaning. It has been known that fuzzy entropy provides information on the uncertainty. However, applying fuzzy entropy theory for fault detection requires greater consideration because of the complementary characteristics [18]. By designing the similarity measure, this difficulty can be resolved. The Hamming distance is usually used to construct the similarity measure. The similarity measure can determine the degree of similarity among data sets. From the following definition of Liu, various similarity measures can be derived.

Definition 3.1 A real function $s: F^2(X) \to R^+$ is called a similarity measure if s has the following properties:

(S1) $s(A,B) = s(B,A), \forall A,B \in F(X)$;

(S2) $s(D,D^c) = 0, \forall D \in P(X)$;

(S3) $s(C,C) = \max_{A,B \in F(X)} s(A,B), \forall C \in F(X)$;

(S4) $\forall A,B,C \in F(X)$, if $A \subset B \subset C$, then $s(A,B) \geq s(A,C)$ and $s(B,C) \geq s(A,C)$.

Using the definition of a similarity measure, we can derive the similarity between fuzzy sets. Consider two Gaussian-type membership functions, as shown in Fig. 3.

In Fig. 3, the area of the shaded region can be considered as a component of the similarity measure. Hence, we express those areas as equations. The two equations $1-d((A\cap B),[1]_X)$ and $1-d((A\cup B),[0]_X)$ will hereafter be denoted as ***C*** and ***D***, respectively. In both these equations, $[1]_X$ and $[0]_X$ are denoted by one and zero for the whole universe of discourse, respectively. ***C*** denotes the common area of a membership function, whereas ***D*** also represents the set information between the two membership functions. ***C*** is equal to one, ***D*** is equal to zero. If ***D*** is equal to one, then the two membership functions are exactly the same. Hence, a proper similarity measure is obtained by combining both the values. We propose a similarity measure that is obtained from a distance measure.

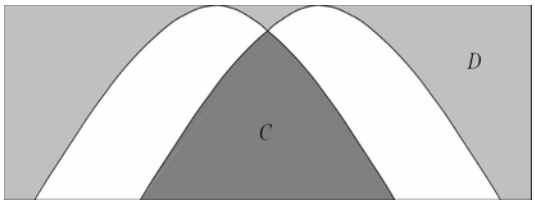

Fig. 3. Gaussian type two fuzzy membership functions.

Theorem 3.1 For any set $A,B \in F(X)$,

$$s(A,B) = 2 - d((A\cap B),[1]_X) - d((A\cup B),[0]_X) \quad (12)$$

is the similarity measure, where d is equal to the Hamming distance.

Proof. In Fig. 3, the summation of the two equations $1-d((A\cap B),[1]_X)$ and $1-d((A\cup B),[0]_X)$ is expressed in terms of common information of two fuzzy sets A and B. If two fuzzy sets are identical, the similarity measure is satisfied for the entire area. Hence, we conjecture that the common information of two fuzzy sets is proportional to the similarity measure. Apparently, the proposed similarity measure is expressed with the area of a distance measure. The usefulness of the proposed similarity measure can be verified by observing whether (12) satisfies Theorem 3.1.

(S1) refers to the commutativity of the sets A and B, which is clear from (12) itself.

For (S2),

$s(D,D^c) = 2 - d((D\cap D^c),[1]_X) - d((D\cup D^c),[0]_X) = 0$

because $d((D\cap D^c),[1]_X)$ and $d((D\cup D^c),[0]_X)$ are equal to one.

For arbitrary different sets A and B, the inequality in (S3) is proved as follows:

$$\begin{aligned} s(A,B) &= 2 - d((A\cap B),[1]_X) - d((A\cup B),[0]_X) \\ &\leq 2 - d((C\cap C),[1]_X) - d((C\cup C),[0]_X) \\ &= s(C,C). \end{aligned}$$

This inequality is satisfied from $d((A\cap B),[1]_X) \geq d((C\cap C),[1]_X)$ and $d((A\cup B),[0]_X) \geq d((C\cup C),[0]_X)$. Finally, $\forall A,B,C \in F(X)$, if $A \subset B \subset C$

$$\begin{aligned} s(A,B) &= 2 - d((A\cap B),[1]_X) - d((A\cup B),[0]_X) \\ &= 2 - d(A,[1]_X) - d(B,[0]_X) \\ &\geq 2 - d(A,[1]_X) - d(C,[0]_X) \\ &= s(A,C). \end{aligned}$$

Further,

$$\begin{aligned} s(B,C) &= 2 - d((B \cap C),[1]_X) - d((B \cup C),[0]_X) \\ &= 2 - d(B,[1]_X) - d(C,[0]_X) \\ &\geq 2 - d(A,[1]_X) - d(C,[0]_X) \\ &= s(A,C) \end{aligned}$$

Two inequalities are satisfied from $d(B,[0]_X) \leq d(C,[0]_X)$ and $d(B,[1]_X) \leq d(A,[1]_X)$. Therefore, $s(A,B) \geq s(A,C)$ and $s(B,C) \geq s(A,C)$ are satisfied. Finally, (S4) is proved.

In the proposed similarity measure, we use the Hamming distance as the distance measure between the fuzzy membership functions A and B. The Hamming distance is commonly used as the distance measure between the fuzzy sets A and B:

$$d(A,B) = \frac{1}{n}\sum_{i=1}^{n} \left| \mu_A(x_i) - \mu_B(x_i) \right|$$

where $X = \{x_1, x_2, \cdots x_n\}$, $|K|$ is the absolute value of K, and $\mu_{\tilde{A}}$ is the membership function of $A \in F(X)$.

For constructing the fuzzy membership function, values of $C_{m_{\delta e}}$, C_{m_α} and C_{L_α} are divided into eight groups, and the number of data sets is normalized. In Fig. 2, it can be observed that the normal and fault values of $C_{m_{\delta e}}$ do not interchange, whereas the normal and fault values of C_{m_α} and C_{L_α} interchange. Hence, it is not easy to obtain an efficient similarity measure with only C_{m_α} and C_{L_α}. Fortunately, $C_{m_{\delta e}}$ helps in distinguishing the operation condition with a remarkable scattering diagram. The fault detection and isolation procedures are schematically shown in Fig. 4. The fault detection procedure involves similarity computation and detection. Similarity computations are performed by using the similarity measure, and the detection part requires more reference data and detailed computation.

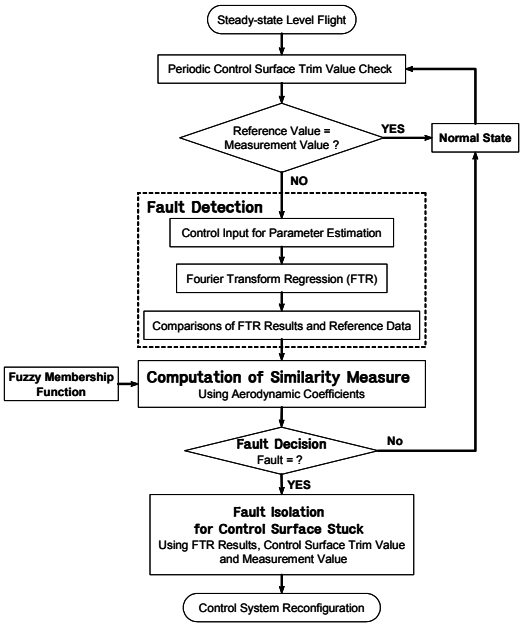

Fig. 4. Fault detection and isolation procedure.

3.3 Fault detection procedure

The normal and fault fuzzy membership functions are illustrated in Fig. 5 by scatter diagrams. From Fig. 2, the maintaining of the control surface stuck by studying the value of coefficients enables the normal and fault states to be easily distinguished. Hence, two fuzzy membership functions are clearly separated with normal and fault membership functions. First, we consider the similarity measure as follows:

$$s_{m_{\delta e}}(F_N, F_F) = 2 - d((F_N \cap F_F),[1]_X) - d((F_N \cup F_F),[0]_X)$$

Here, F_N and F_F denote the normal and fault fuzzy membership functions shown in Fig. 5.

However, the coefficients C_{m_α} and C_{L_α} are mixed; therefore, determining the normal and fault states from C_{m_α} and C_{L_α} may lead to confusion. At this point, we propose a similarity measure involving $C_{m_{\delta e}}$, C_{m_α} and C_{L_α}. Further, we also propose another similarity measure involving C_{m_α} and C_{L_α}:

$$s_{m_\alpha}(F_N, F_F) = 2 - d((F_N \cap F_F),[1]_X) - d((F_N \cup F_F),[0]_X)$$

and

$$s_{L_\alpha}(F_N, F_F) = 2 - d((F_N \cap F_F),[1]_X) - d((F_N \cup F_F),[0]_X) .$$

Six data points are selected from Fig. 2 (c) to calculate and analyze the characteristics. Points **a** - **f** of C_{L_α} are also listed in Fig. 2 (c) as follows:

a = 4.9974, **b** = 5.6780, **c** = 5.7549,
d = 5.5991, **e** = 5.56238, and **f** = 5.4462.

The six points are located in the common area between the normal and the fault conditions. To determine the similarity measure, the corresponding membership values are also necessary; therefore, the

membership values of point **a** shown in Fig. 5 are considered.

From these similarity measures, the mixed similarity measure is obtained as follows:

$$s(F_N,F_F)=\omega_1 s_{m_{\delta e}}(F_N,F_F)+\omega_2 s_{m_\alpha}(F_N,F_F)+\omega_3 s_{L_\alpha}(F_N,F_F) \quad (13)$$

where ω_1,ω_2, and ω_3 are the weighting factors for the similarity measure. From (13), we calculate the tendency of occurrence of normal or fault cases for six points. The values of $s_{m_{\delta e}}(F_N,F_F)$ are classified into normal and fault cases on the basis of $s_{m_{\delta e}}(F_N,\mathrm{p})$ and $s_{m_{\delta e}}(\mathrm{p},F_F)$ for fault point **p**. Similarly, the other similarities $s_{m_\alpha}(F_N,F_F)$ and $s_{L_\alpha}(F_N,F_F)$ are also classified from **a** to **f**.

In Table 4, we notice that the similarity measures for the 3-fault cases **a**, **b,** and **c** are greater than the normal similarity measures. This implies that the fault decisions are obtained by similarity computation and comparison. Furthermore, three normal cases are found to be correctly detected. By using the mixed similarity measure in (13), we assign the values of ω_1, ω_2, and ω_3 to be one. Fortunately, points **a** - **f** of C_{L_α} are easily classified because of the clear membership function of $C_{m_{\delta e}}$. If the membership functions of the parameters have varying significance with respect to their values, we use the proper tuning of ω_1, ω_2 and ω_3.

In Fig. 2, we have illustrated the case of an elevator with 50 % failure; in the figure, we can notice that the effectiveness of the elevator has decreased, and the occurrence of a fault cannot be identified from the scatter diagram, especially Fig.2 (a), even though the data group is closed. If an aircraft has a 20~30 % control surface loss as damage during a battle, it can be assumed that this can lead to a decrease in value of $C_{m_{\delta e}}$ by up to nearly 20~30 %. Then, the scatter data $C_{m_{\delta e}}$ shown in Fig. 2 (a) are closed and mixed, and fault detection becomes more difficult. In such a case, the similarity measure helps in detecting the fault. Furthermore, the weighting parameters ω_1,ω_2, and ω_3 are also used for proper detection. The corresponding

Table 4. Computation of similarity measure.

	a (fault)	**b** (fault)	**c** (fault)	**d** (normal)	**e** (normal)	**f** (normal)
$s_{m_{\delta e}}(F_N,\mathrm{p})$	0	0	0	0.77	0.77	0.54
$s_{m_{\delta e}}(\mathrm{p},F_F)$	1	1	1	0	0	0
$s_{m_\alpha}(F_N,\mathrm{p})$	0	0.42	0.83	0.83	1	0.42
$s_{m_\alpha}(\mathrm{p},F_F)$	1	0.73	0.62	0.64	0.23	0.73
$s_{L_\alpha}(F_N,\mathrm{p})$	0.67	1	1	1	1	1
$s_{L_\alpha}(\mathrm{p},F_F)$	0.74	1	1	1	1	1
$s(F_N,\mathrm{p})$	0.67	1.42	1.83	**2.60**	**2.77**	**2.73**
$s(\mathrm{p},F_F)$	**2.74**	**2.73**	**2.62**	1.64	1.23	1.73

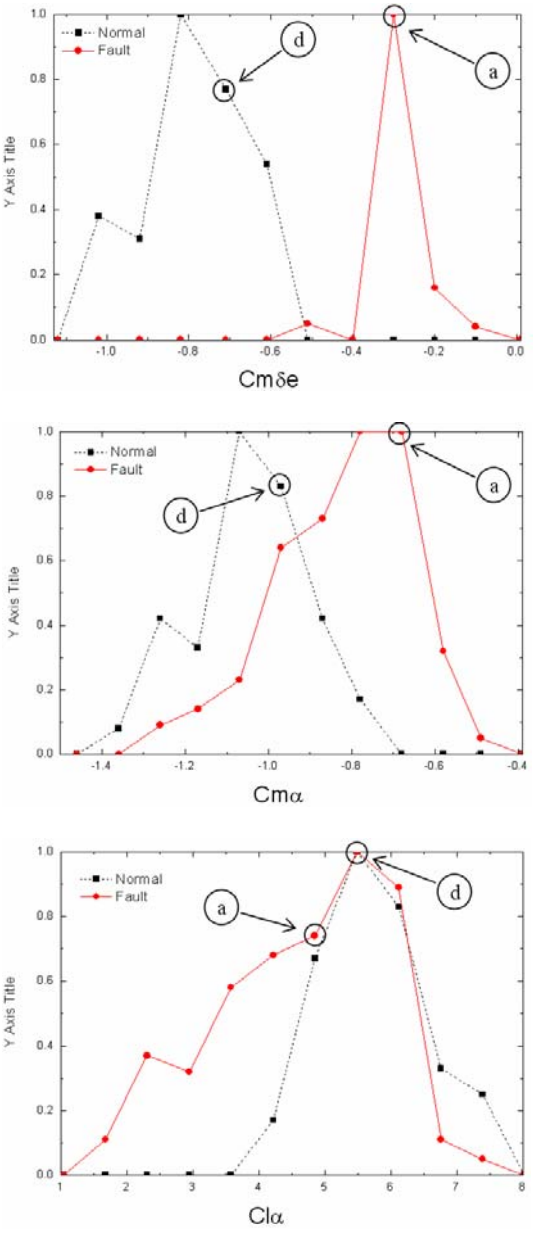

Fig. 5. Membership function of $C_{m_{\delta e}}$, C_{m_α}, and C_{L_α} coefficients.

fuzzy membership functions of $C_{m_{\delta e}}$, C_{m_α}, and C_{L_α} are shown in Fig. 5. From the scatter diagram shown in Fig. 2 (a), the fuzzy membership function of $C_{m_{\delta e}}$ is found to be clearly separated.

To determine the fault state and the normal state and to find the control surface that it seems not to operate, the FCC detects and isolates the control surface fault by using the procedure shown in Fig. 4. In flight, the FCC periodically checks the measured trim value against the reference value in a steady-state level flight. If the measured value is considerably different from the error limit, the FCC applies the control input for the real-time parameter estimation. The FCC isolates the control surface failure by comparing the estimated coefficients with the reference coefficients. The FCC determines the control surface stuck position by comparing the trim value with the reference value. Fault detection and isolation by using the real-time parameter estimation method helps in studying the differences between the trim values and the variations in the aerodynamic coefficients. With the aid of the real-time parameter estimation of the normal and fault operations through the simulation of aerodynamic coefficients, it can be recognized that the control surface fault is detected by variations in the coefficients [3-4]. Fault detection from the flight test data is difficult because the normal and fault operation data are scattered and mixed with each other.

4. Conclusions

In this study, we examined the normal mode and fault mode with the right elevator stuck, the left rudder stuck, the left aileron stuck, and the combination of these. It is confirmed that the faults can be detected by monitoring the value of the roll damping derivative (C_{l_p}) and the coefficients of the control surface deviation $C_{m_{\delta e}}$. It is found that the control surface stuck position is determined by comparing the trim value with the reference value. If an aircraft has 20~30 % control surface loss, the scatter of $C_{m_{\delta e}}$ is nearly closed and the fault detection is more difficult than this study case. With the help of the similarity measure, faults or normal conditions can be detected; the similarity measure makes a clear and easy distinction between the faults and normal conditions. Even for mixed data, it is expected that desirable results can be obtained by tuning the weighting values. Furthermore, if the flight control system is reconfigured using the online estimates of the aircraft parameters by using a real-time parameter estimation scheme, an increase in the reliability is achieved without the cost of providing a sensor, such as a potentiometer on the control surface or for additional modification.

References

[1] Y. K. Song, A Study on Real-Time Aircraft Parameter Estimation, *Proc. of the KSAS Spring Annual Meeting*, (2001) 359-362.

[2] Y. D. Kim, A Study on Fault Detection and Redundancy Management System, SUDP-P1-G4, March (2005).

[3] M. R. Napolitano, Y. K. Song and B. Seanor, Online parameter estimation for restructurable flight control systems, Aircraft Design, 4 (2001) 19-50.

[4] M. R. Napolitano, S. Naylor, C. Neppach and V. Casdorph, Online Learning Nonlinear Direct Neurocontrollers for Restructurable Control Systems, *Journal of Guidance, Control, and Dynamics*, 18 (1) (1996) 170-176.

[5] S. H. Lee, H. J. Park and W. J. Park, Similarity computation between fuzzy set and crisp set with similarity measure based on distance, *LNCS*, 4993 (2008) 644-649.

[6] Liu, X., Entropy, distance measure and similarity measure of fuzzy sets and their relations, *Fuzzy Sets and Systems,* 52 (1992) 305-318.

[7] J. L. Fan and W. X. Xie, Distance measure and induced fuzzy entropy, *Fuzzy Set and Systems*, 104 (1999) 305-314.

[8] M. S. Hwang, W. J. Park, et al., Lateral Stability Improvement of a Canard Airplane Using a Vertical Panel, *AIAA Atmospheric Flight Mechanics Conference and Exhibit*, AIAA-2002-4625, Monterey, California (2002).

[9] M. S. Hwang, H. B. Eun, W. J. Park, et al., Lateral Stability/Control Derivatives Estimation of Canard Type Airplane from Flight Test, *Proc. of the ICCAS* (2001).

[10] W. J. Park, W. T. Kim, K. J. Seong and Y. C. Kim. A Study on the Parameter Estimation of DURUMI-II for the Fixed Right Elevator Using Flight Test Data, *Journal of Mechanical Science and Technology*, 20 (8) (2006) 1224-1231.

[11] R. C. Nelson, *Flight Stability and Automatic Control*, McGraw-Hill, NY(1998) 96-127.

[12] E. A. Morelli, High Accuracy Evaluation of the Finite Fourier Transform Using Sampled Data,

NASA-TM-110340, (1997).
[13] E. A. Morelli, In-flight System identification, *Proc. of the 1998 AIAA Atmospheric Flight Mechanics Conference*, AIAA-98-4261, Boston, MA, (1998).
[14] E. A. Morelli, Real-Time Parameter Estimation in the Frequency Domain, *Proc. of the 1999 AIAA Atmospheric Flight Mechanics Conference*, AIAA-99-4043, Portland, Or. (1999).
[15] E. A. Morelli, Identification of Low Order Equivalent System Models From Flight Test Data, NASA-TM-210117, (2000).
[16] W. J. Park, A Study on the Design of Real-Time Parameter Estimator for an Aircraft, *PhD Thesis*, Hankuk Aviation University, (2004).
[17] W. J. Park, E. T. Kim, Y. K. Song and B. J. Ko, A Study on the Real-Time Parameter Estimation of DURUMI-II for Control Surface Fault using Flight Test Data, *International Journal of Control, Automation, and Systems*, 5 (4) (2007) 410-418.
[18] S. H. Lee, Y. Y. Kim, S. P. Cheon and S. S. Kim, Reliable Data Selection with Fuzzy Entropy, *LNCS*, 3613 (2005) 203-212.

Wook-Je Park received the B.S. and the Ph.D. degrees, both in Aeronautical Engineering, from Korea Aerospace University in 1994 and 2005, respectively. He is now a Post-Doc in Mechanical and Aeronautical Engineering, Western Michigan University. His research interests are in fault detection and isolation, real-time parameter estimation method, flight test, and their application in aircraft and UAV.

Sang-Hyuk Lee received the Ph. D. degree in Electrical Engineering from Seoul National University in 1998. Dr. Lee has been with the Changwon National University as a research professor since 2006. His research interests include fuzzy theory, game theory, and nonlinear control.

Jung-Il Song received his Ph. D. degree in Mechanical Engineering from POSTECH, Korea, in 1997. Dr. Song is currently a Professor at the School of Mechanical Engineering at Changwon National University in Changwon, Korea. His research interests include manufacturing process and evaluation of composites, biomedical engineering and rehabilitation engineering.